ELSEVIER

Magnetic Resonance Materials in Physics, Biology and Medicine 13 (2001) 15–18

MAGMA

Magnetic Resonance Materials in Physics, Biology and Medicine

www.elsevier.com/locate/magma

# Spectroscopic imaging of bone marrow composition in vertebral bodies

Jan Weis [a,b,*], Ipek Ciray [a], Anders Ericsson [a], Henrik Lindman [a], Gunnar Åström [a], Håkan Ahlström [a], Anders Hemmingsson [a]

[a] *Department of Oncology, Radiology and Clinical Immunology, Uppsala University Hospital, Uppsala, Sweden*
[b] *Institute of Measurement Science, Slovak Academy of Sciences, Bratislava, Slovakia*

Received 29 August 2000; received in revised form 15 December 2000; accepted 9 January 2001

**Abstract**

The proton spectroscopic imaging technique that uses read gradient during acquisition was used for the measurement of the proton spectra in the lumbar and thoracic part of the spine of a patient with breast cancer without known skeletal metastases. The bone marrow fat water ratios were evaluated in the same location before and after chemotherapy treatment. The results were corrected for relaxation effects. The fat/water ratios showed a significant increase as a consequence of the bone marrow degradation process due to chemotherapy. The proposed spectroscopic imaging technique offers rapid acquisition of proton spectra from large volumes of the vertebral bodies. © 2001 Elsevier Science B.V. All rights reserved.

*Keywords:* Spectroscopic imaging; Fat–water proton spectroscopy; Bone marrow; Chemotherapy

## 1. Introduction

In hematological or metabolic diseases, the composition of the bone marrow can alter during chemo- and radiotherapy. During and after the treatment the red marrow can change to yellow marrow and vice versa. Since the amount of fat in red marrow ($\sim 40\%$) is much less than the amount of fat in yellow marrow ($\sim 80\%$) in adolescents [1,2], non-invasive measurement of the water and fat content by MR techniques may give a measure of the red/yellow marrow ratio. To obtain more detailed information about the bone marrow composition it is necessary to separate the contributions of fat and water. Several methods have been used to accomplish this goal. One method uses phase interference effects to measure the fat/water ratio in trabecular structure of vertebral bodies [3]. Another group of methods used chemical shift imaging [4,5]. A third approach to assess alternations of the bone marrow is volume-selective $^1$H-spectroscopy [6–9] and magnetic resonance spectroscopic imaging (MRSI) [10,11].

We have applied a variant of the MRSI technique that uses read gradient during acquisition [12,13]. This method permits measurement of the proton spectra with high spatial and moderately high spectral resolution with acquisition times of some minutes. The volume of interest (VOI) can be defined flexibly to conform with irregularly shaped vertebral bodies. The advantage of spectroscopic imaging with high spatial resolution is the post-detection definition of relatively large and irregularly shaped VOI. This possibility has an important significance in reliable characterization of bone marrow structure, for example in the spine, where red and yellow marrow distribution is heterogeneous [7].

## 2. Materials and methods

A 52-year-old female breast cancer patient with no clinical or biochemical signs of skeletal metastases was investigated. The proton spectra were recorded with a Philips (Best, The Netherlands) Gyroscan NT whole-

* Corresponding author. Present address: MTA/RTG, Ing. 85, 2 Tr., University Hospital, SE-751 85 Uppsala, Sweden. Tel.: +46-18-61113765; fax: +46-18-503622.
*E-mail address:* jan.weis@mta.uas.lul.se (J. Weis).

1352-8661/01/$ - see front matter © 2001 Elsevier Science B.V. All rights reserved.
PII: S1352-8661(01)00119-3

body imager working at 1.5 T. The whole body coil was used for excitation and receiving. The spectroscopic imaging technique with high spatial resolution was based on a radiofrequency (RF) spoiled fast gradient echo sequence ($TR = 100$ ms, $\alpha = 25°$) [13,14]. The spectral information was encoded by incrementing the echo time $TE_m = TE_1 + m\Delta T$ of the subsequent 32 image records ($m = 0, 1, 2...31$) with $TE_1 = 9$ ms, FOV = 450 mm, slice thickness 5 mm, (256, 256) image matrix and chemical shift artefact two pixels; 192 phase encoding steps (scan percentage 75%) and one acquisition was used. Incrementing the echo time by $\Delta T = 1.56$ ms led to a spectral bandwidth of 10 ppm (640 Hz). The spectral resolution was 0.31 ppm (19.8 Hz). The net measurement time was 10.2 min. Oversampling factor 2 was used in read gradient direction $k_{read}$. Data processing were performed on a Sun Ultra 10 workstation (Sun Microsystems Inc., CA, USA). The measured matrix ($k_{read}$, $k_{phase}$, $m$) = (512, 192, 32) was zero-filled before data processing to a complex matrix size (512, 256, 256). The first Fourier transform was performed along the $m$ axis. The data matrix was then corrected for chemical shift artefacts using a first-order phase correction [13,14]. Data processing continued by spatial 2D Fourier transform in the read ($k_{read}$) and phase-encoding dimensions ($k_{phase}$). Oversampling of the data matrix was removed during the Fourier transform along the $k_{read}$ axis. The resulting matrix ($x_{read}$, $y_{phase}$, $\sigma$) of the size (256, 256, 256), where $x_{read}$, $y_{phase}$ are spatial co-ordinates and $\sigma$ is the shielding constant, represents the proton spectra in a given voxel ($1.76 \times 1.76 \times 5$ mm$^3$) of the measured slice. Complex proton voxel spectra were then simplified to the magnitude spectra. The static magnetic field distribution $\Delta B(x_{read}, y_{phase})$ in the measured slice was computed from the shift of the highest spectral peak in each voxel and used to reshift the voxel spectra about $\Delta B(x_{read}, y_{phase})/B_0$ along the spectral axis $\sigma$ [13,14]. The chemical shift artefact-free image (Fig. 1a) was computed by integration of the water and fat voxel spectral peaks. An integration range of $\pm 0.3$ ppm ($\pm 19$ Hz) over the water and fat spectral lines was used. The chemical shift artefact-free image served for definition of the volume of interest. The selection was performed manually with the aid of a 'light pen'. The typical VOI in vertebral bodies ($\sim 1550$ voxels, 24 cm$^3$) is depicted by overlaid high intensity pixels in Fig. 1a. The average magnitude spectrum per voxel from the defined group of the voxels (VOI) was calculated by summation of the individual voxel spectra and division by the number of voxels. Subtraction of a constant was used for baseline correction.

The spectra were analyzed by a standard peak-fitting procedure. Two Lorentzian shaped curves were used to fit the water (4.8 ppm) and fat ($-CH_2-)_n$ (1.6 ppm) peaks (see dotted curves in Fig. 1b). Due to limited spectral resolution the lipid spectrum was not analyzed in more detail. Signal intensity I was computed from the area of the Lorentzian fitted water ($I_w$) and fat ($I_f$) spectral lines and used for evaluation of the fat/water spin density ratio ($I_f/I_w$). In principle, signal intensities are directly proportional to concentrations, the proportionality constant is the same for all the spectral lines.

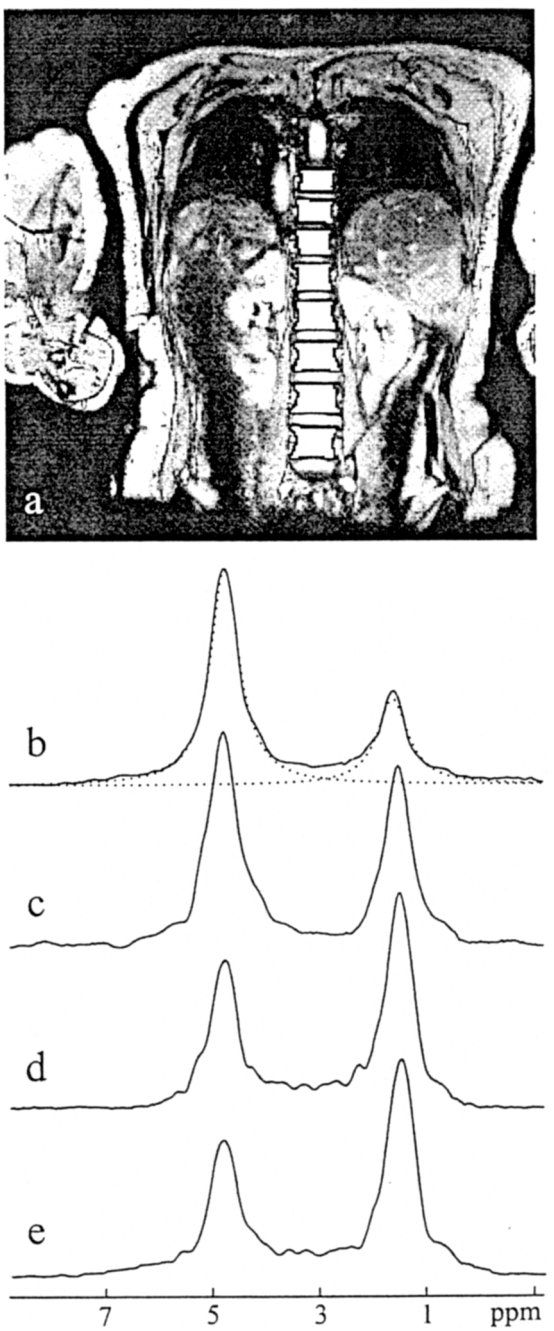


Fig. 1. The average proton spectra of the lumbar and thoracic part of the spine. (a) The irregularly shaped VOI in the vertebral bodies ($\sim 1550$ voxels, 24 cm$^3$) is depicted by overlaid high intensity pixels. (b) Normal spectrum before the beginning of chemotherapy. The dotted curve displays the fitted Lorentzian line. (c) Spectrum just after 8 months course of the chemotherapy. (d) Spectrum 2 months after finishing the treatment. (e) Spectrum 7 months after end of chemotherapy.

However, effects related to relaxation have to be taken into account for quantitative results [15]. The steady state signal achieved for RF spoiled fast gradient echo sequence can be described by the following well-known equation [16]:

$$I = \rho \frac{[1 - \exp(-TR/T_1)]\sin(\alpha)}{[1 - \exp(-TR/T_1)]\cos(\alpha)} \exp(-TE/T_2^*) \qquad (1)$$

where ρ is proton density. Eq. (1) corresponds to the situation where the transverse magnetization before the next excitation pulse is effectively spoiled and cannot rephase at a later time [17]. The relaxation corrected water $\rho_w$ and fat $\rho_f$ spin densities were computed using Eq. (1) with $TE = TE_1$ where $TE_1$ is the echo time of the first image record, i.e. time of the first point of the $k$-FID [13,18]. In the calculation of the water $\rho_w$ (red bone marrow) and fat $\rho_f$ (yellow bone marrow) spin densities, spin–spin relaxation values $T_{1w} = 1350$ ms for water and $T_{1f} = 290$ ms for fat were used [8]. The effective spin–spin relaxation time of water $T_{2w}^* = 12.2 \pm 0.3$ ms and fat $T_{2f}^* = 14.1 \pm 0.4$ ms were computed from the full width half maximum (FWHM) ($T_2^* = \sqrt{3}/(\pi * \text{FWHM})$) of the Lorentzian shaped curves which were used for fitting of the magnitude spectra (Fig. 1b–e) [19]. These values agree well with the literature value $T_2^* = 13.4 \pm 1.3$ referring to the lumbar spine of a 48-year-old healthy subject [20]. The spin density fat/water ratio $\rho_f/\rho_w$ was then converted to fat/water weight ratio $m_f/m_w$ using formulas $m_f = \frac{267.8}{24.5}\rho_f$ and $m_w = \frac{18}{2}\rho_w$ where 267.8 g/mol and 18 g/mol are the molecular weight of triglycerides and water, respectively. Constants 24.5 and 2 are average numbers of protons in the triglyceride that exist as $(-CH_2-)_n$ and water, respectively. This calculation is based on the well-known fact that the lipid composition of human bone marrow consists almost exclusively from the triglycerides [7,10].

## 3. Results

The proton spectra in the lumbar and thoracic part of the spine (Fig. 1a) were measured in the same location before and after chemotherapy. Fig. 1b shows a normal $^1$H-spectrum before starting the chemotherapy. The amplitude of the water peak (4.8 ppm) is approximately two times higher than the fat peak (1.6 ppm). The measured fat/water spectral line intensities $I_f/I_w$ and fat/water weight ratio $m_f/m_w$ were 0.48 and 0.29, respectively (Table 1). Fig. 1c shows the spectrum just after the 8-month course of therapy was completed. The fat/water signal intensity ratio increased to 0.74 and fat/water weight ratio to 0.45. Increase of the fat/water ratio continued even 2 months after the end of treatment (Fig. 1d). The fat/water signal intensity and weight ratios reached values of 1.25 and 0.76, respectively. The last measurement (Fig. 1e) was performed 15 months after beginning the treatment (7 months after finishing the chemotherapy). Relatively small increase of the fat/water signal intensity (1.48) and weight ratio (0.90) indicated a slowing down of the bone marrow degradation process.

Table 1
Fat/water signal intensity, spin density[a] and weight ratios[a]

| Time (months) | Fat/water signal intensity ratio $I_f/I_w$ (a.u.) | Fat/water[a] spin density ratio $\rho_f/\rho_w$ (a.u.) | Fat/water[a] weight ratio $m_f/m_w$ (a.u.) |
|---|---|---|---|
| 0 | 0.48 | 0.24 | 0.29 |
| 8 | 0.74 | 0.37 | 0.45 |
| 10 | 1.25 | 0.63 | 0.76 |
| 15 | 1.48 | 0.74 | 0.90 |

First row (0 month) shows fat/water ratios before the beginning of chemotherapy. Second row (8 months) contains values just after the treatment. Rows 3 (10th month) and 4 (15th month) shows fat/water ratios 2 and 7 months after finishing the chemotherapy. Error ± 16% was estimated for the values corrected for relaxation effects.

[a] Corrected for relaxation effects.

## 4. Discussion

In post-detection data processing the voxel spectra were corrected for the shifts caused by the static magnetic field deviations. Good quality of the proton spectra could therefore be obtained without shimming procedures. Voxel spectra summation allowed an enhancement of the signal-to-noise ratio ($S/N$). However, this summation is relatively inefficient in terms of sensitivity: the $S/N$ in the sum of $N$ voxels is reduced by $\sqrt{N}$ compared to the signal from an $N$-times larger volume [13]. The calculations of the fat/water weight ratios suffers from the fact that the peak areas have to be corrected for relaxation effects. The computed effective relaxation times of water $T_{2w}^* = 12.2 \pm 0.3$ ms and fat $T_{2f}^* = 14.1 \pm 0.4$ ms are probably sufficiently reliable [20]. However, the relaxation time $T_1$ of water and fat in bone marrow of the vertebral bodies displays large variations [4,6,8]. The spin-lattice relaxation time of water $T_{1w}$ was found in a range between 1000 and 1700 ms, and $T_{1f}$ (fat) in a range between 260 and 320 ms in healthy volunteers. The quantitative results corrected for relaxation effects (Table 1) have therefore limited precision. The error ± 16% for relaxation corrected values (Table 1) was estimated by varying the mean $T_{1w} = 1350$ ms value approximately ± 300 ms and $T_{1f} = 290$ approximately ± 30 ms.

The spectrum quality of the described spectroscopic imaging method is inferior to those obtained by the usual single voxel (PRESS, STEAM) sequences [6–9]. $S/N$ and spectral linewidths are, however, comparable.

The disadvantage of single voxel spectroscopy is longer total measurement time due to shimming procedures, measurement of anatomic images and manual definition of VOI before spectrum measurement. The advantage of spectroscopic imaging with high spatial resolution is post-detection definition of large and irregularly shaped VOI. This has an important significance in view of the fact, that the distribution of red and yellow marrow is very heterogeneous within each vertebral body and between different vertebrae [7]. The described technique can be useful to study the ratio between red and yellow bone marrow during treatment of patients with various bone marrow disorders.

## 5. Conclusions

The spectroscopic imaging method offers rapid acquisition of proton spectra from large volumes. The short examination time, the post-detection definition of the irregularly shaped VOI and the fact that there is no shimming or special hardware requirements, makes the technique easily applicable in practice.

## Acknowledgements

Financial support by the Swedish Medical Research Council, Project No. K2000-73X-13154-02B, K2000-73X-06676-18E and Swedish Society of Medicine is gratefully acknowledged. We express our gratitude to Johan van den Brink (Philips, Best) for writing the patch pulse sequence.

## References

[1] Higgins CB, Hricak H, Helms CA. Magnetic resonance imaging of the body, 3rd ed. New York: Lippincott-Raven Press, 1997:1295.

[2] Vogler JB, Murphy WA. Bone marrow imaging. Radiology 1988;168:679–93.

[3] Derby K, Kramer DM, Kaufman L. A technique for assessment of bone marrow composition using magnetic resonance phase interference at low field. Magn Reson Med 1993;29:465–9.

[4] Rosen BR, Fleming DM, Kushner DC, Zaner KS, Buxton RB, Bennet WP, et al. Hematologic bone marrow disorders: Quantitative chemical shift MR imaging. Radiology 1988;169:799–804.

[5] Schick F, Bongers H, Jung WI, Skalej M, Lutz O. Localized Larmor frequency-guided fat and water proton MRI of the spine: A method to emphasize pathological findings. Magn Reson Imaging 1991;9:509–15.

[6] Jensen KE, Jensen M, Sorensen PG, Thomsen C, Karle H, Henriksen O. Localized in vivo proton spectroscopy of the bone marrow in patients with leukemia. Magn Reson Imaging 1990;8:779–83.

[7] Schick F, Bongers H, Jung WI, Skalej M, Lutz O, Claussen CD. Volume-selective proton MRS in vertebral bodies. Magn Reson Med 1992;26:207–17.

[8] Schick F, Bongers H, Jung WI, Eismann B, Skalej M, Einsele H, et al. Proton relaxation times in human red bone marrow by volume selective magnetic resonance spectroscopy. Appl Magn Reson 1992;3:947–63.

[9] Schick F, Einsele H, Kost R, Duda SH, Horny HP, Lutz O, et al. Localized MR $^{1}$H spectroscopy reveals alterations of susceptibility in bone marrow with hemosiderosis. Magn Reson Med 1994;32:470–5.

[10] Richards TL, Davis CA, Barker BR, Beinert WD, Genant HK. Lipid/water ratio of bone marrow measured by phase-encoded proton nuclear magnetic resonance spectroscopy. Invest Radiol 1987;22:741–6.

[11] Mulkern RV, Meng J, Bowers JL, Oshio K, Zuo CH, Li H, et al. In vivo bone marrow lipid characterization with line scan Carr–Purcell–Meiboom–Gill proton spectroscopic imaging. Magn Reson Imaging 1997;15:823–37.

[12] Matsui S, Sekihara K, Kohno H. High-speed spatially resolved high-resolution NMR spectroscopy. J Am Chem Soc 1985;8:585–7.

[13] Weis J, Ericsson A, Hemmingsson A. $^{1}$H-spectroscopic imaging with read gradient during acquisition in inhomogeneous fields: analysis, measurement strategy, and data processing. MAGMA 1997;5:201–12.

[14] Weis J, Ericsson A, Hemmingsson A. Chemical shift artefact-free microscopy: Spectroscopic imaging of the human skin. Magn Reson Med 1999;41:904–8.

[15] De Certaines JD, Bovée WMM, Podo F. Magnetic resonance spectroscopy in biology and medicine. Oxford: Pergamon Press Ltd, 1992.

[16] Mansfield P, Morris PG. NMR imaging in biomedicine. New York: Academic Press, 1982.

[17] Van Der Meulen P, Groen JP, Tinus AMC, Bruntink G. Fast field echo imaging: an overview and contrast calculations. Magn Reson Imag 1988;6:355–68.

[18] Twieg DB, Katz RM, Peshock RM. A general treatment of NMR imaging with chemical shifts and motion. Magn Reson Med 1987;5:32–46.

[19] Marshall AG, Verdun FR. Fourier transform in NMR, optical, and mass spectrometry. Amsterdam: Elsevier Science Publishers BV, 1990.

[20] Wehrli FW, Ford JC, Attie M, Kressel HY, Kaplan FS. Trabecular structure: Preliminary application of MR interferometry. Radiology 1991;179:615–21.